JOURNAL OF MATERIALS SCIENCE 20 (1985) 3101 – 3110

The effect of filler particle size and orientation on the impact fracture toughness of a highly filled plasticized polymeric material

C. W. FONG, R. C. WARREN
Weapons Systems Research Laboratory, Defence Research Centre Salisbury, GPO Box 2151, Adelaide, South Australia 5001, Australia

The effect of particle size and orientation on the inherent fracture toughness of a filled plasticized polymeric material has been determined by application of linear elastic fracture mechanics. Testing was caried out in a three-point bend mode under impact conditions. The material was a triple base gun propellant consisting of a matrix of nitrocellulose plasticized with nitroglycerine and filled with particles of nitroguanidine (NQ). The crystalline NQ was used in the "as-received" form of needles and in a "ground" state. The material containing as-received NQ consistently had a higher fracture toughness than the material with ground NQ, and the toughness was a maximum when the fillers were aligned perpendicularly to the fracture surface. The impact fracture toughness was found to be virtually independent of strain rate over the range from 3 to 90 sec^{-1}.

Seven-perforated cylindrical grains of the material containing as-received and ground NQ crystals, and the grains were tested in a pneumatic gas gun and a Hopkinson bar apparatus. The grains containing the ground NQ have been shown to be generally less resistant to fracture than the grains containing as-received NQ.

1. Introduction

It has been known for some time that M30 type triple base propellant can give rise to anomalous ballistic performance at both low and high temperatures during gun firings. It has been suggested that the low-temperature ballistic anomalies result from propellant grain fracture induced by non-ideal ignition of the propellant bed [1, 2]. In these circumstances the propellant bed is driven forwards so that the grains at the leading edge of the bed strike the projectile base at high velocities, thereby causing grain fracture.

The propellant is an example of a highly filled, plasticized polymeric composite. The impact strength of polymers containing fillers is a subject of much interest owing to the role played by the filler and its interface with the polymer [3]. However, there are few studies of the high strain rate impact behaviour of plasticized highly filled systems, and especially there is a paucity of data on the influence of filler size, shape and orientation.

This study investigates the high strain rate impact fracture behaviour of an extruded highly filled plasticized polymer as a function of filler size, shape and orientation in both the bend and compressive modes.

2. Experimental procedure

2.1. Formulation and extrusion

The composition (wt %) was: nitrocellulose (NC), 28.0; nitroglycerine (NG), 22.5; nitroguanidine (NQ), 47.7; ethyl centralite, 1.5; cryolite, 0.3. The nitrogen level of the NC was 12.6%.

0022–2461/85 $03.00 + .12

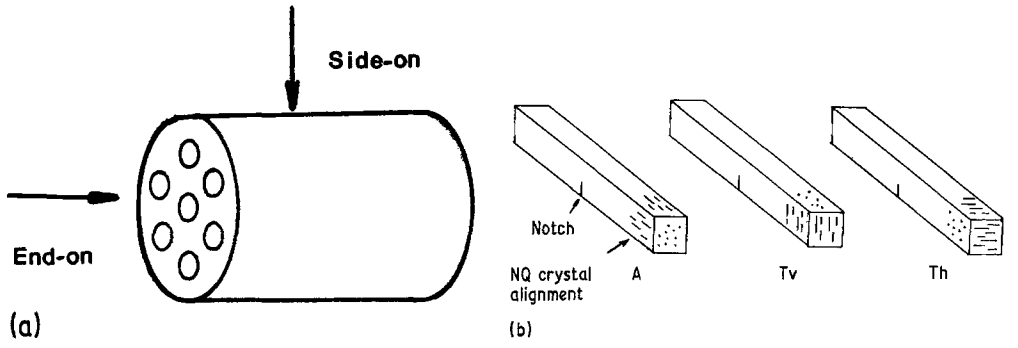

Figure 1 (a) Schematic representation of grain geometry and testing directions. (b) Schematic representation of the three impact specimen types and their relationship with the orientation of the NQ crystals.

The material containing as-received NQ was designated ARNQ. Similarly the material containing ground nitroguanidine was designated GNQ. To make the ground NQ, the as-received NQ was ground in a Sweco mill for 5 h using freon as a dilutent. The average length/diameter ratios of the needle-like crystals of the as-received NQ were about 15:1 to 25:1 and after grinding were about 2:1 to 3:1 (though there were a small number of crystals whose ratios were about 5:1 to 6:1). The average particle size of the GNQ was about 3 to 5 μm.

Specimens for instrumented drop weight impact testing were either extruded as bars from a 9.5 mm square die or as slabs from a 30 mm × 8 mm rectangular die. The resultant material was then machined into specimen bars of dimensions 30 mm × 6 mm × 6 mm, 45 mm × 6 mm × 6 mm and 80 mm × 6 mm × 6 mm. The absolute densities of a number of specimen bars of the ARNQ and GNQ material were determined to be indentical within error (1.667 ± 0.003 g cm^{-3}).

Specimens for pneumatic gas gun and Hopkinson bar testing were extruded through a die 9.8 mm in diameter with seven pins 1 mm in diameter aligned in the axial direction and symmetrically spaced in cross-section. The resulting cord was cut to give grains of the form illustrated in Fig. 1. The average grain dimensions (in millimeters) for the ARNQ and GNQ material respectively were: length, 19.1 and 18.7; diameter, 8.15 and 8.49; outer web, 1.50 and 1.58; inner web, 1.36 and 1.46; outer perforations, 0.83 and 0.79; centre perforations, 0.81 and 0.87.

2.2. Instrumented drop weight impact testing

The impact testing was carried out on a Dynatup Model 8200 Instrumented Drop Weight Tester linked to an ETI 300 data aquisition system (Effects Technology Inc, Santa Barbara). The specimens were tested in a three-point bend mode, and the impact load was monitored by strain gauges on the tup.

The extrusion process produced a strong alignment of the as-received filler particles along the extrusion direction, which was confirmed by examination of fracture surfaces by scanning electron microscopy (SEM). To test the effect of particle alignment, bars 30 mm × 6 mm × 6 mm were machined from slabs. Specimens with the bar axis parallel to the filler alignment, or the extrusion direction, were designated ARNQ/A or GNQ/A, and specimens with the bar axis transverse to the filler alignment were designated ARNQ/T or GNQ/T. These orientations are illustrated in Fig. 1.

Specimen bars were carefully notched with fresh razor blades to a depth of 0.5 mm at dry ice temperatures. For ARNQ/T bars, there are two possible orientations of the filler particles with respect to the notch, as illustrated in Fig. 1. The alignment of the filler parallel to the notch front is designated ARNQ/Th, and the alignment of the filler perpendicular to the notch front is designated ARNQ/Tv. Similarly the GNQ bars were designated GNQ/Th and GNQ/Tv to indicate whether the notch was parallel or perpendicular to the extrusion axis, to correspond to the ARNQ specimens.

The fracture surfaces for a representative

number of specimens were examined with a calibrated low-powered microscope to check the notch depth accurately and to assess the type of fracture. Generally a nominal notch depth of 0.5 mm resulted in an actual notch depth of 0.55 mm.

Specimens were preconditioned for at least 30 min at the required temperature (in a carbon dioxide-cooled conditioning chamber) before testing. The time between removal from the conditioning chamber and completion of the test was not greater than 30 sec. The test temperatures used were -60, -45, -30, -15, 0 and 20° C.

For the major part of this study, two standard test spans of 24 and 36 mm were used for the 30 mm × 6 mm × 6 mm and 45 mm × 6 mm × 6 mm specimens respectively, and the impact velocity was 0.5 m sec^{-1}. The effect of strain rate was determined at 0 and -60° C by using an additional span of 72 mm for the 80 mm × 6 mm × 6 mm bars, and also using additional impact velocities of 1.0 and 1.5 m sec^{-1}. Each datum point of integrated fracture energy, or maximum load at fracture, for a particular orientation and temperature was the average of three to five separate tests. Generally, the reproducibility of these tests was within 10%.

The inertial oscillations in the tup gave rise to "ringing" of the load signal. The oscillations were generally not excessive and were averaged out by obtaining the best-fit straight line. Such a procedure has good theoretical and instrumental justification [4].

The fracture toughness, K_c, values [5] were determined from:

$$K_c = Y\sigma a^{1/2}$$

where Y is a geometrical factor previously determined for several geometries, σ is the maximum gross stress and a is the initial notch depth. The maximum stress, σ, is calculated [6] from:

$$\sigma = 3P(S/2)BD^2$$

where P is the maximum load at fracture, and S, B and D are the span, breadth and depth of the test specimen.

2.3. Pneumatic gas gun testing

Graphite-coated grains containing ARNQ and GNQ were conditioned for at least 30 min at the required temperatures. The grains were then removed and transferred to the gas gun barrel (which is also conditioned at the required temperature) and fired within 1 min. The test temperatures were -40, -10, 20 and 50° C, and the impact velocities were 70, 90 and 110 m sec^{-1}.

The three basic impact modes were: (1) square end-on impact (Mode A), (2) end-on impact at an angle (Mode B), and (3) side-on impact (Mode C). The mode of impact was determined by coating the target with a thin film of white stencil ink and examining the impact surface for signs of graphite. For each particular temperature and velocity, firings were continued until at least ten impacts for both Modes A and B were recorded.

2.4. Hopkinson bar compression testing

In Hopkinson bar compression testing the specimen is mounted on a stationary bar which is instrumented with strain gauges to measure applied load. A moving bar is fired at the specimen, which is compressed between the two bars. The displacement of the moving bar and the load on the stationary bar are used to calculate load–displacement curves for the impact on the specimen. A description of the technique is given elsewhere [7].

Seven-perforated axisymmetric cylinders (8 mm diameter by 8 mm length) of ARNQ and GNQ material were machined from standard grains. The load–time and displacement–time curves were recorded on a Nicolet 4094 digital oscilloscope. The specimens were conditioned for at least 30 min at the required temperatures, mounted quickly on the output bar and tested (usually within 30 to 60 sec). The specimens were mounted on the bar with grease, and the impact surfaces were also lightly greased to reduce surface frictional effects. The impact velocities used covered the range from 5 to 25 m sec^{-1}. The test temperatures used in the study were -40, -10, $+20$ and $+50$° C. Individual specimens were accurately dimensioned prior to testing. The specimens were tested in two modes: (a) side-on and (b) end-on, as shown in Fig. 1. Three specimens were tested at each set of conditions, and the reproducibility was generally within 15%.

3. Results and discussion

3.1. Instrumented drop weight impact testing

The test data for the ARNQ and GNQ materials

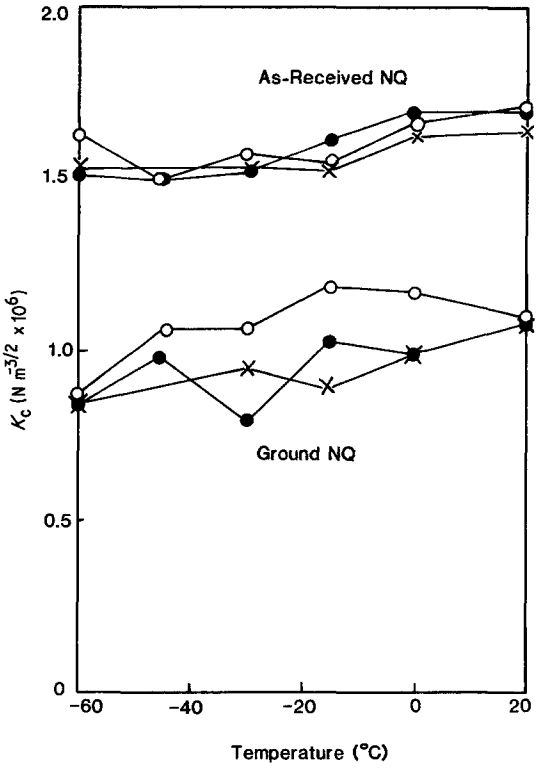

Figure 2 K_c against temperature for ARNQ and GNQ with specimen axis along NQ crystal direction: ●, specimen from bar, 24 mm span; ○, specimen from slab, 24 mm span; ×, specimen from bar, 36 mm span.

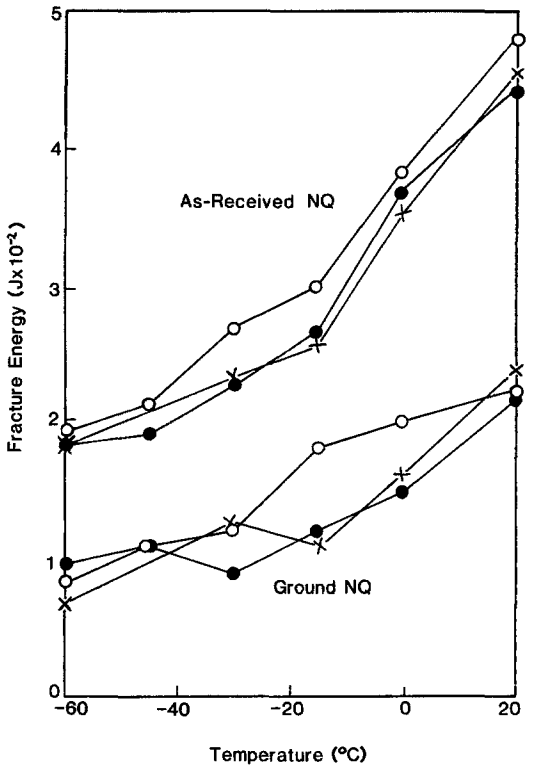

Figure 3 Fracture energy against temperature for ARNQ and GNQ with specimen axis along NQ crystal direction: ●, specimen from bar, 24 mm span; ○, specimen from slab, 24 mm span; ×, specimen from bar, 36 mm span.

were analysed in terms of the fracture toughness, K_c, and the integrated fracture energy. The majority of specimens were machined from the extruded slabs, and were tested with a 24 mm test span. A lesser number were machined from the extruded bar and were tested with 24 and 36 mm test spans to evaluate possible span effects. From an examination of SEM micrographs of the fracture surfaces of ARNQ and GNQ materials, it was observed that the longer needles of as-received NQ were more regularly oriented along the extrusion direction in the ARNQ material than were the ground NQ crystals in the GNQ material.

The fracture surfaces of ARNQ/A specimens with the fillers aligned along the bar axis, i.e. across the fracture surface, were typically more jagged and rough than any of the other specimen types. ARNQ/T specimens with the fillers aligned transversely to the bar axis, i.e. parallel to the fracture surface, showed the next roughest fracture surfaces. Surfaces from GNQ specimens were uniformly the smoothest of all the surfaces. The fracture surfaces that were most square (as opposed to those that were slightly angled or slanted) were generally the smoothest surfaces. Specimens whose fracture surfaces deviated badly from orthogonality to the notched face of the specimen were disregarded in the final analysis.

The principal conclusions to emerge from this study are:

(a) The ARNQ material is substantially more resistant to impact fracture than is the GNQ material when tested with the fillers aligned along the specimen axis. In this case the fracture surface is perpendicular to the extrusion direction. Fig. 2 shows a plot of K_c against temperature for ARNQ/A and GNQ/A specimens machined from slabs and tested over a span of 24 mm, and specimens machined from the extruded bars and tested over spans of 24 and 36 mm. Fig. 3 shows a plot of fracture energy against temperature for the same tests. Generally the trends in fracture toughness, as indicated by K_c, were paralleled by the trends in fracture

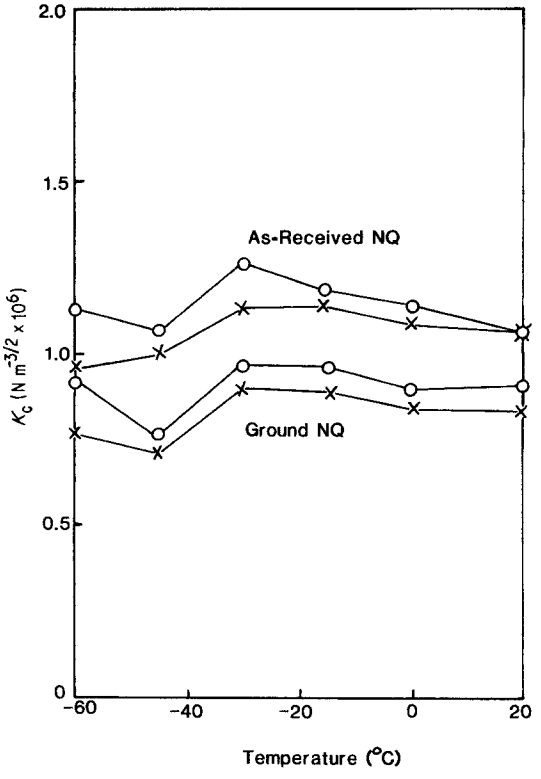

Figure 4 K_c against temperature for ARNQ and GNQ with specimen axis transverse to NQ crystal direction. Specimens from slab, 24 mm span: ○, Tv direction; ×, Th direction.

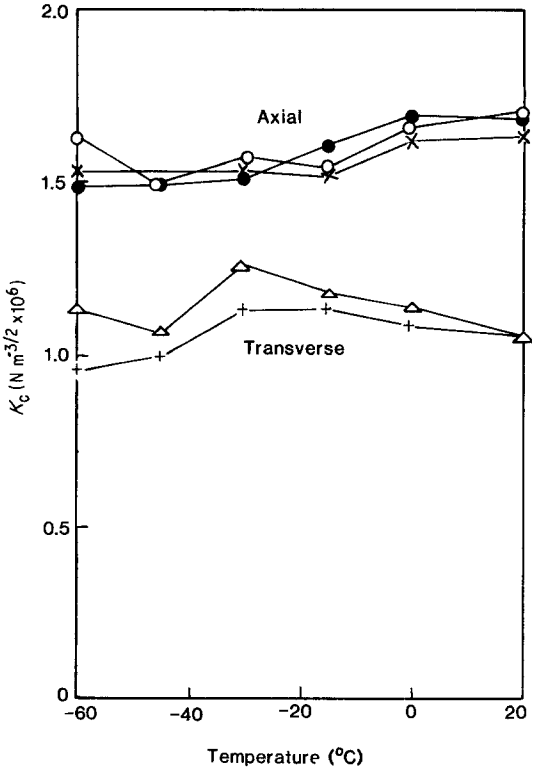

Figure 5 K_c against temperature for ARNQ. Specimens from bar: ●, 24 mm span; ×, 36 mm span. Specimens from slab: ○, axial; +, Tv; △, Th.

energy for all impact testing carried out in this study. The differences between the results from specimens of different lengths and specimens cut from the slab and the bar are negligible and within experimental error. The effect of test span is also negligible.

(b) The ARNQ material is more resistant to fracture than is the GNQ material when tested with the extrusion direction aligned transversely to the specimen axis in either the horizontal, h, or vertical, v, direction. In this case the fillers area aligned parallel to the fracture surface. Fig. 4 plots the values of K_c of specimens of ARNQ/Th, GNQ/Th, ARNQ/Tv and GNQ/Tv. The differences in K_c were reflected in the relative smoothness of the fracture surfaces.

(c) The ARNQ material is more resistant to fracture when tested with the fillers aligned along the specimen axis than when tested with the fillers aligned transversely to the specimen direction, as shown in Fig. 5. This result is also in agreement with qualitative observations of the two types of fracture surface. The effect of test span appears to be negligible.

(d) The material GNQ is equally resistant to fracture when tested either with the specimen axis parallel to the extrusion direction, GNQ/A, or transversely to the extrusion direction, GNQ/T, as shown in Fig. 6. Thus the ground NQ crystals do not confer any orientation effects, with respect to fracture toughness, on the material. The fracture surfaces appeared to be equally smooth for the axial, A, and transverse, T, test modes. The effect of test span appears to be negligible.

K_c appears to be independent of temperature change, and fracture energy shows only a small dependence on temperature change (see Figs. 2 to 6).

(e) The effect of strain rate on K_c was determined at 0 and $-60°$ C using spans of 24, 36 and 72 mm, and impact velocities of 0.5, 1.0 and 1.5 m sec^{-1}. The strain rate was varied between 3 and 90 sec^{-1}. At low values of strain rate the inertial oscillations in the tup were small, and accurate values of K_c could be determined. However, at the higher strain rates the duration of the test approached the period of the tup

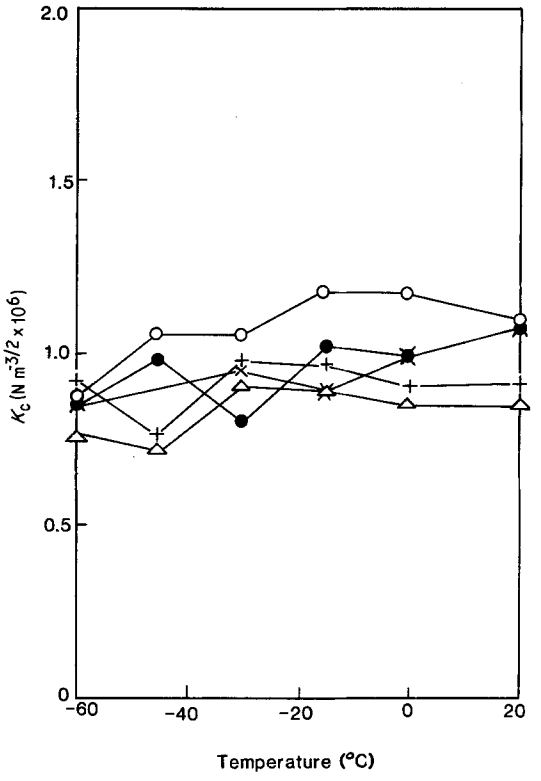

Figure 6 K_c against temperature for GNQ. Specimens from bar: ●, 24 mm span; ×, 36 mm span. Specimens from slab: ○, axial; +, Tv; △, Th.

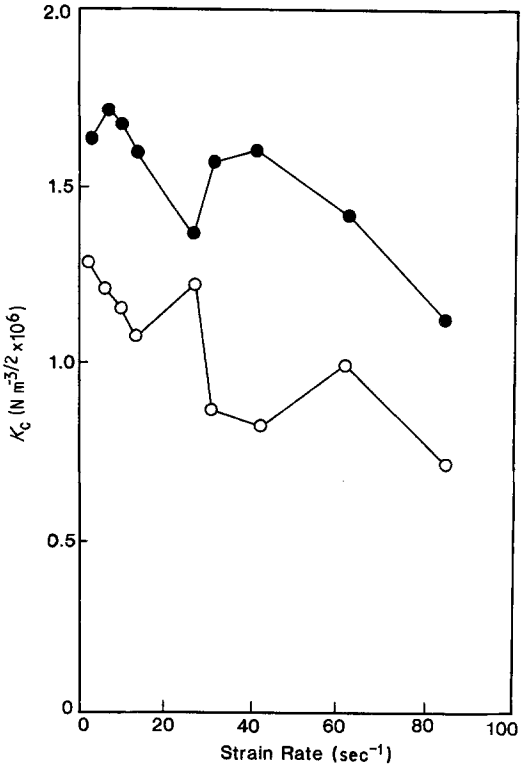

Figure 7 K_c against strain rate at 0° C: ●, ARNQ; ○, GNQ.

oscillation, and hence the tup probably would not have responded sufficiently quickly to the applied load. The load value recorded, and hence the calculated K_c, would then be somewhat less than the actual values involved [8]. The −60° C data were particularly affected. The measured values of K_c are plotted against strain rate in Figs. 7 and 8. It can be seen from the figures that the effect of strain rate on K_c over the range studied is quite small. Such a result is in accord with the apparent insensitivity of K_c with temperature noted above (Figs. 2, 4, 5 and 6), indicating the existence of a time–temperature relationship.

3.2. Pneumatic gas gun testing

The severity of fracture was assessed visually on a six-point scale: 0, largely undamaged; 1, slight cracking only, usually around the perforations or periphery of the grain; 2, greater cracking accompanied by chipping; 3, longitudinal splitting; 4, longitudinal splitting and severe chipping; and 5, complete shattering. All rankings were done as consistently as possible by one assessor. An arbitrary test of the consistency of

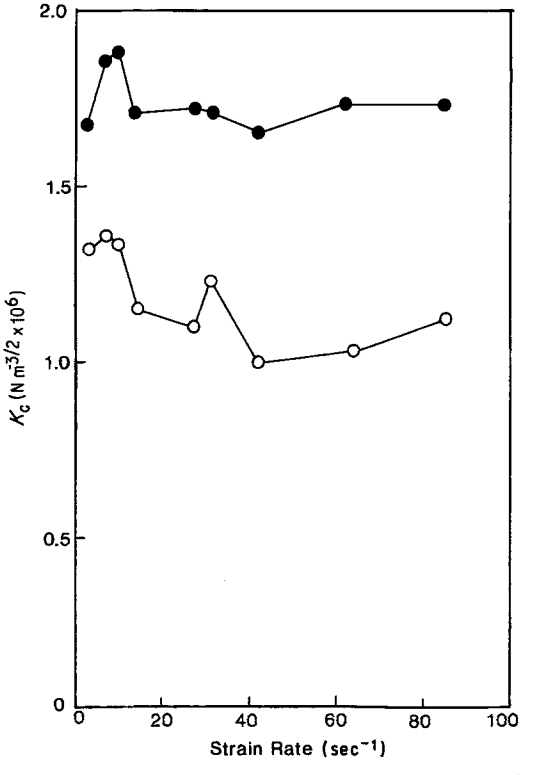

Figure 8 K_c against strain rate at −60° C: ●, ARNQ; ○, GNQ.

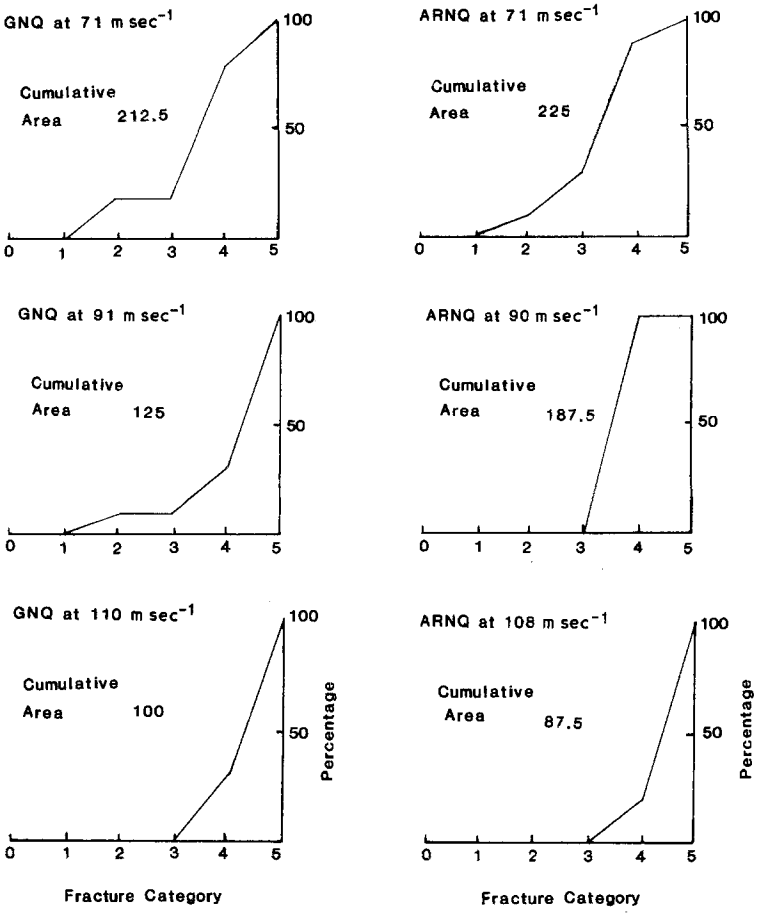

Figure 9 Cumulative frequency diagrams for fracture of ARNQ and GNQ grains when fired in the gas gun.

this procedure (especially for Categories 2 to 5) was conducted by weighing the larger fracture remnants. This test gave results in good accord with the visual assessment procedure.

In this study, most impacts were Mode A, end-on impact, or Mode B, end-on at a small angle. The few Mode C, side-on, impacts that occurred indicated a greater degree of break-up than occurred with Mode A or B type impacts under comparable conditions.

The fracture results for a particular temperature and velocity are presented as cumulative frequency diagrams, as shown in Fig. 9. The area under the curve is defined as the fracture resistance. A cumulative area value of 625 is obtained with 100% of the sample in Category 0, and a value of 62.5 is obtained with 100% of the sample in Category 5. The velocity spread for a nominal velocity (e.g. 70, 90 or 110 m sec^{-1}) was generally no more than ± 3 m sec^{-1}.

In Fig. 10, both Type A and B impacts have been summed for the velocities 70, 90 and 110 m sec^{-1}, and temperatures of -40, -10, 20 and 50° C. At all velocities, the ARNQ material is clearly more resistant to fracture than the GNQ material. From Fig. 10, it can be seen that both materials become increasingly brittle at lower temperatures and higher velocities (the same conclusion can be seen if fracture resistance is plotted against velocity for a constant temperature). An observation of obvious importance was that both materials showed a greatly increased propensity to shatter when the grains impacted the target side-on.

3.3. Hopkinson bar compression testing

In the side-on tests, all the specimens shattered completely into small fragments. The size of the fracture fragments from the GNQ grains was generally slightly larger than that from the ARNQ grains, especially in the lower-velocity ranges (5 to 8 m sec^{-1}).

For end-on tests in the impact velocity range

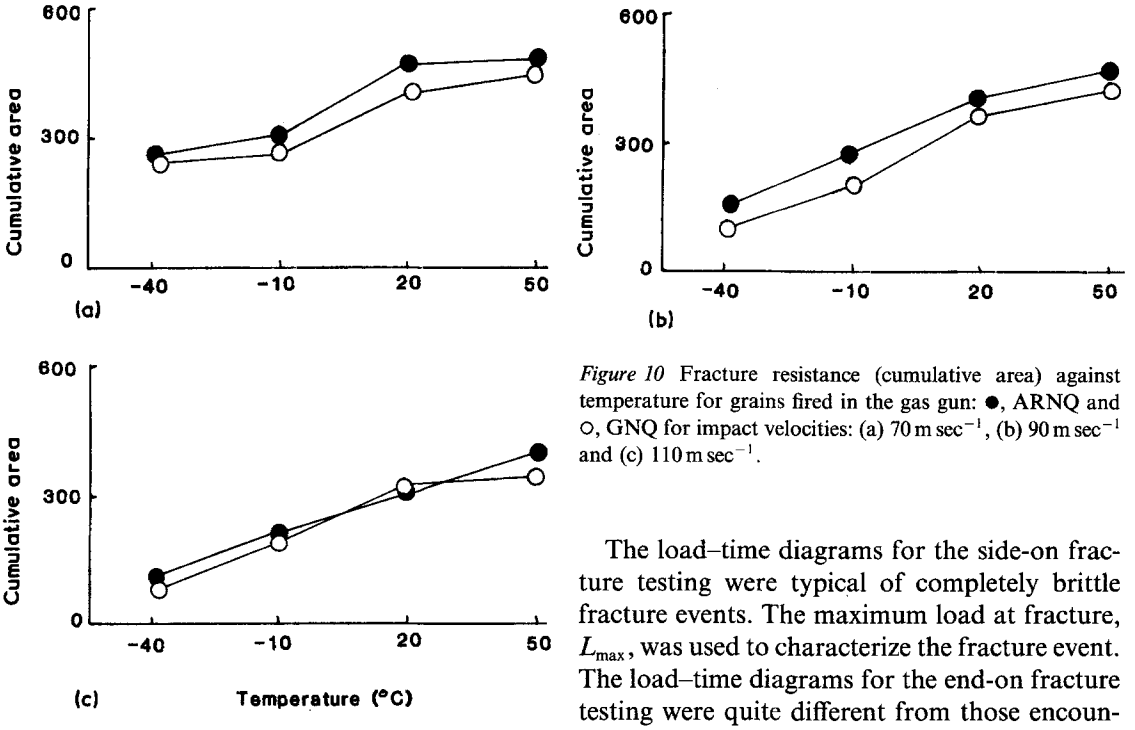

Figure 10 Fracture resistance (cumulative area) against temperature for grains fired in the gas gun: ●, ARNQ and ○, GNQ for impact velocities: (a) 70 m sec^{-1}, (b) 90 m sec^{-1} and (c) 110 m sec^{-1}.

5 to 8 m sec^{-1}, none of the specimens shattered completely, but they were flattened to varying degrees with small cracks around the perforations and peripheries of the grains. In the range 14 to 17 m sec^{-1}, specimens from the ARNQ grains shattered completely into small particles, whereas specimens of the GNQ grains were generally severely flattened with many large cracks. In the range 22 to 25 m sec^{-1}, all the ARNQ and GNQ samples shattered completely.

The load–time diagrams for the side-on fracture testing were typical of completely brittle fracture events. The maximum load at fracture, L_{max}, was used to characterize the fracture event. The load–time diagrams for the end-on fracture testing were quite different from those encountered in the side-on testing, as shown in Fig. 11. The curves for end-on impacts were characterized by an initial linear region up to the point, L_{fo}. This point has been taken to be the load at fracture onset (L_{fo}), since inspection of specimens impacted at the lower velocities showed evidence of small cracks around the perforations and peripheries of the grains (such specimens showed only minor overall dimensional changes before and after compression testing). It is recognized that the point L_{fo} can only represent

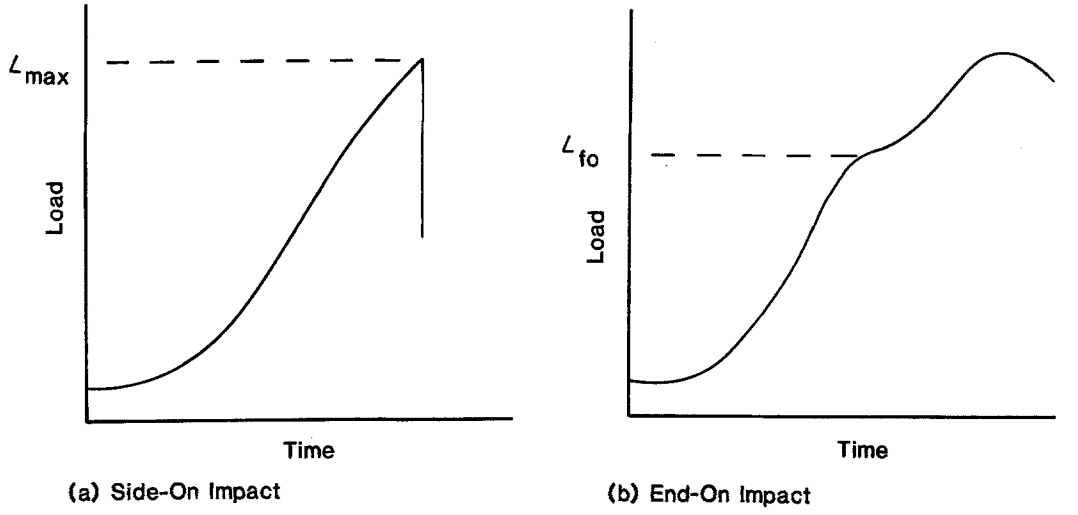

Figure 11 Load–time diagrams for typical fractures of grains on the Hopkinson bar.

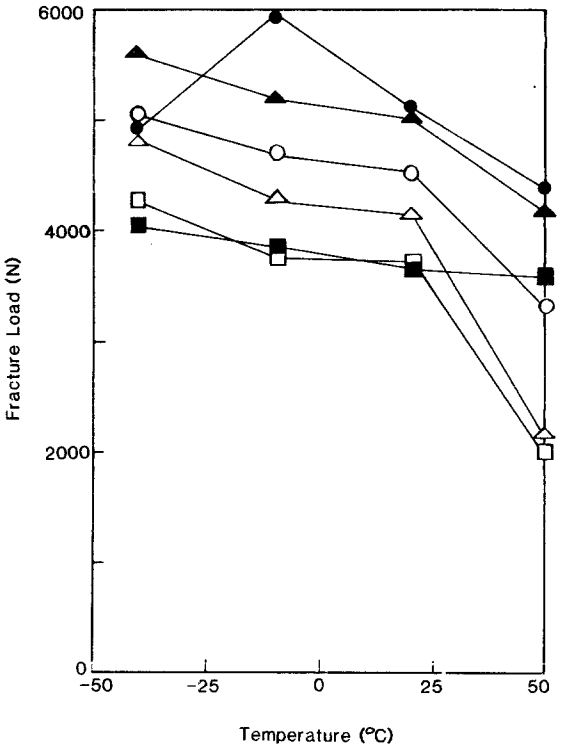

Figure 12 Fracture load, L_{fo}, against temperature for end-on impacts on the Hopkinson bar: filled points, ARNQ; open points, GNQ; ●, ○, 23 to 25 m sec^{-1}; ▲, △, 15 to 18 m sec^{-1}; ■, □, 4 to 10 m sec^{-1}.

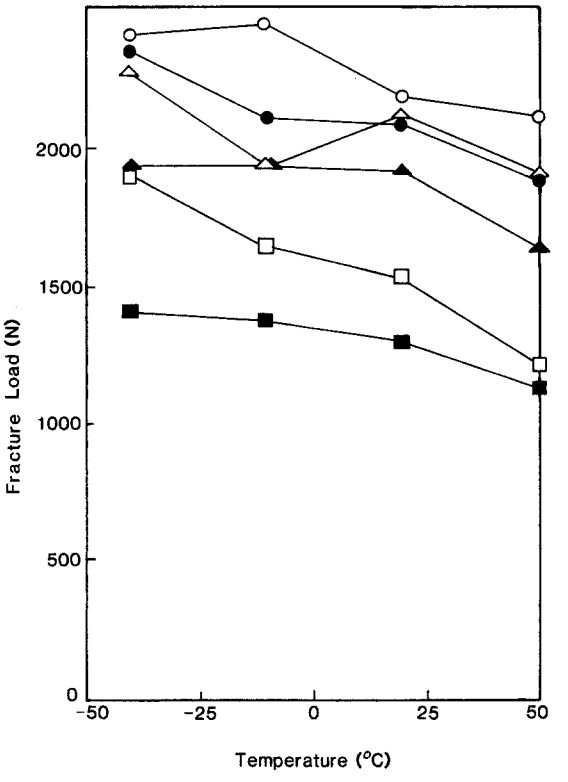

Figure 13 Fracture load L_{max}, against temperature for side-on impacts on the Hopkinson bar: filled points, ARNQ; open points, GNQ; ●, ○, 23 to 25 m sec^{-1}; ▲, △, 15 to 18 m sec^{-1}; ■, □, 4 to 10 m sec^{-1}.

the onset of fracture which is experimentally detectable; minor cracking could occur before L_{fo}. Figs. 12 and 13 illustrate L_{max} and L_{fo} for side-on and end-on impacts on ARNQ and GNQ material at -40, -10, 20 and 50° C for the three impact velocity ranges, 4 to 7, 14 to 18 and 23 to 25 m sec^{-1}.

The following conclusions can be drawn:

(a) End-on impacts: With two minor exceptions (at -40° C), it can be seen from Fig. 12 that ARNQ material has a larger value of L_{fo} than the GNQ material. Also, in the range 14 to 17 m sec^{-1}, the degree of fragmentation exhibited by the ARNQ material is significantly greater than that shown by the GNQ material.

(b) Side-on impacts: From Fig. 13, it can be seen that the GNQ material has a higher value of L_{max} than the ARNQ material. This trend is most marked in the low-velocity range, 4 to 10 m sec^{-1}. The data also indicate that at the lowest temperature and highest velocities, both materials are approaching a similar brittle fracture limit.

4. Conclusions

In this study, we have investigated the impact fracture behaviour of triple base M30 type propellant containing as-received NQ and ground NQ. The ARNQ and GNQ materials have been studied in the form of notched rectangular bars, regular seven-perforated axisymmetric grains (the normal ballistic configuration) and as machined seven-perforated axisymmetric cylinders. Thus three conceptually different test modes were used to evaluate the fracture toughness of the materials: three-point impact bending of notched bars; high-velocity impact of regular grains against a target plate; and high-strain rate compression of machined cylinders of material.

In testing notched bars of material, we are primarily testing the inherent fracture toughness of the material itself, free from geometrical stress constraints imposed by the seven-perforated axisymmetric cylindrical shape of the regular grains. K_c, the fracture toughness, is a true material parameter [5].

The conclusions are quite clear:

(a) Propellant containing as-received NQ (ARNQ) is more fracture-resistant than material containing ground NQ (GNQ) when tested either with the specimen axis along the direction of NQ crystal orientation (or direction of extrusion) or when tested at right angles to the direction of NQ crystal orientation.

(b) ARNQ material is more fracture-resistant when tested along the direction of orientation of the NQ crystals than when tested at right angles to the crystal orientation.

(c) GNQ material is equally resistant to fracture when tested either along or at right angles to the direction of extrusion.

(d) The fracture toughness is largely independent of strain rate over the strain rate range 3 to 90 sec^{-1}.

Gas gun testing of regular grains of ARNQ and GNQ material indicates that the ARNQ material is more resistant to fracture than the GNQ material when the grains are impacted squarely end-on or end-on at an angle. No extensive data are available for side-on impacts.

When specimens are compressed end-on in the Hopkinson bar, the ARNQ material can sustain a greater load before fracture than the GNQ material. However, in the side-on mode, the specimens of GNQ material exhibit greater fracture resistance than the ARNQ material. It is interesting to note that the gas gun impact results (for end-one specimens) appear to agree with the Hopkinson bar results although they are quite different in principle. With the exception of the side-on Hopkinson bar data, it appears that the ARNQ material is more resistant to fracture than the GNQ material.

The results from the fracture of notched bars of material can obviously be expected to differ from the fracture results obtained by gas gun or Hopkinson bar testing, because these results reflect the inherent fracture toughness of the material only. The particular geometry (i.e. axisymmetric seven-perforated cylinders) into which this material is cast, as well as the inherent fracture toughness of the material, will be the final arbiters of how that particular specimen will resist fracture.

References

1. R. LANTZ and A. J. BEARDELL, International Jahrestagung (ICT, Karlsruhe, Germany, 1982) p. 639.
2. C. W. FONG and B. K. MOY, *J. Ballistics* **6** (1982) 1410.
3. L. E. NIELSEN, "Mechanical Properties of Polymers and Composites" (Marcel Dekker, New York, 1974) Ch. 7.
4. S. VENZI, A. H. PRIEST and M. J. MAY, ASTM Special Technical Publication 563 (American Society for Testing and Materials, Philadelphia, 1974) p. 170.
5. J. E. SRAWLEY, "Fracture", Vol. 4, edited by H. Leibowitz (Academic Press, New York, 1969), Ch. 2.
6. G. P. MARSHALL, J. G. WILLIAMS and C. E. TURNER, *J. Mater. Sci.* **8** (1973) 949.
7. G. T. WULF and G. T. RICHARDSON, *J. Phys. E: Sci. Instrum.* **7** (1973) 167.
8. W. R. HOOVER, ASTM Special Technical Publication 563 (American Society for Testing and Materials, Philadelphia, 1974) p. 203.

Received 6 June
and accepted 20 September 1984